

Broadband tunable hybrid photonic crystal-nanowire light emitter

Christophe E. Wilhelm, M. Iqbal Bakti Utama, Gaëlle Lehoucq, Qihua Xiong, Cesare Soci, Daniel Dolfi, Alfredo De Rossi and Sylvain Combrié,

Abstract—We integrate about 100 single cadmium selenide semiconductor nanowires in silicon nitride photonic crystal cavities in a single processing run. Room temperature measurements reveal a single and narrow emission linewidth, corresponding to a Q-factor as large as 5000. By varying the structural parameters of the photonic crystal, the peak wavelength is changed, thereby covering the entire emission spectral range of the active material. A very large spectral range could be covered by heterogeneous integration of different active materials.

Index Terms—photonic crystal, semiconductor nanowires, nano-lasers, optical cavity.

INTRODUCTION

The miniaturization of laser devices [1] is crucial in the context of on-chip optical communications, but also for medical imaging or sensing [2]. Furthermore, scaling down the size of the laser source reduces the power consumption as the active volume is decreased [3], [4]. This is a critical issue when a massive number of emitters of a small volume is meant to coexist in a tiny space. A third implication is an intrinsically faster response [1]. However, the available gain is reduced when down-sizing the active volume; therefore it is crucial to associate the emitter to a small but high quality optical cavity.

In surface-plasmon based cavities the optical confinement breaks the diffraction limit, hence allowing an extremely large enhancement of the light-matter interaction. In this regime, the optical field oscillates by exchanging its energy with electrons in the metal, where Joule effect induces a very fast decay [5]. While this is not an issue in the context of fast extraction through enhanced stimulated emission [6], it compromises the goal of energy-efficient light emission, particularly in the visible and near the infrared spectral domain.

A close to diffraction limited confinement is possible in dielectric cavities based on the Bragg scattering, e.g. Photonic Crystals (PhC), still keeping optical losses to a very low level [7]. Thus, a continuous wave laser operating at room temperature has been demonstrated [8] by combining a very

small active area with a high-quality PhC cavity. These lasers have been heterogeneously integrated on a silicon chip [9], [10] and the technology is, in principle, able to address the challenge of massive integration.

The concept of heterogeneous integration can be pushed further so that the active material, e.g. a nanowire (NW) [11] or a colloidal quantum dot [12], which are synthesized in large number, is integrated into a passive dielectric structure and, ultimately, in a complex photonic circuit. A single III-V nanowire has been inserted into a silicon PhC waveguide, which creates an optical cavity self-aligned with the emitter [13]. The heterogeneous integration on silicon chip is an important result. Also, the complexity and the criticality of the manufacturing process are reduced, as the fabrication of the active material and of the photonic chip are independent. The most critical issue, however, remains the deterministic alignment of the active nano-object with the optical resonator. This was initiated for achieving strong coupling regime between a single QD and a PhC cavity [14], [15].

In this paper, we create a self-aligned cavity by inserting a single CdSe nanowire into a silicon nitride Photonic Crystal. By mapping the NW positions by topographic Atomic Force Microscopy measurements, and accurately constructing PhCs around the NWs rather than manually aligning them individually, we demonstrate fabrication of about one hundred heterogeneous devices at the same time, with substantially equivalent optical functionality. Each of these devices emits a narrow photoluminescence peak which is deterministically controlled by adjusting the structural parameters of the PhC, thereby addressing the whole spectral range of the active material.

DEVICE DESIGN

The device concept is shown in Fig.1. The starting point is a PhC waveguide made of silicon nitride (Si_3N_4). Within the spectral range of interest, there is only one guided mode, with the dispersion represented in Fig.1a. The dispersion is red-shifted by the addition of a NW which increases the effective refractive index locally. This creates an effective potential well for the optical field inducing a resonance (Fig 1b) and a localized mode (Fig 1c), spectrally centred within the edges of the two bands in Fig 1a. The corresponding field distribution is well localized around the nanowire, in spite of the weaker index contrast available.

This point as been thoroughly addressed in a recent paper

Christophe E. Wilhelm is with the Department of School of Electrical and Electronic Engineering, Nanyang Technological University, 639798 Singapore and also with CINTRA (CNRS International NTU THALES Research Alliance), 639798 Singapore.

M. Iqbal Bakti Utama, Qihua Xiong and Cesare Soci are Division of Physics and Applied Physics, School of Physical and Mathematical Sciences, Nanyang Technological University, 637371 Singapore.

Gaëlle Lehoucq, Daniel Dolfi, Alfredo De Rossi and Sylvain Combrié are with Thales Research and Technology, 91767 Palaiseau France

Manuscript received December 1, 2016; revised XXXX XX, XXXX.

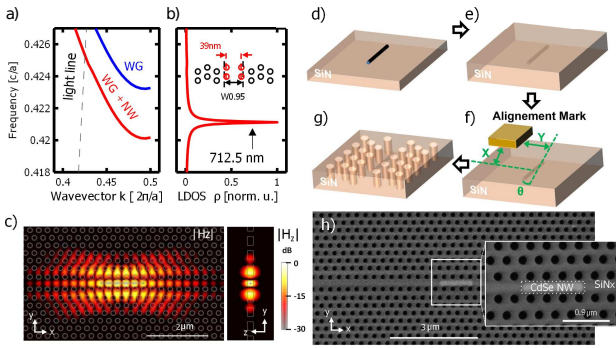


Fig. 1. Concept of the PhC-NW cavity: calculated dispersion of the PhC waveguide with (red) and without NW (blue) a) and, b), Local Density of States (normalized) peak ($Q=5300$); the inset represents the design of the PhC WG; distribution of the magnetic field $|H_z|$ at the resonance, represented as a false-color map in logarithmic scale c). Fabrication process flow of the PhC-NW source d-g). Deposition of SiN_x on the substrate d); NW dispersion and deposition of the SiN_x cladding layer e); Localization of the NW by AFM f); patterning of the PhC aligned to the NW g) prior to the local removal of the substrate; Scanning Electron Micrograph from the top of the PhC suspended membrane with a magnified view in the inset h).

[16]. The main outcome is that the symmetric design, such as that used here, is preferable. That article also illustrates that the design of such structures is much more challenging using SiN compared to larger index material such as silicon. Another issue is the impact of misalignment, which is also discussed there. In any case, the average accuracy of alignment which we achieve is such that misalignment is not the limiting factor for the Q factor. Fluctuations in the parameters of the NW and, on top of that, the fact that they are rather thick and short, is the main factor preventing the achievement of larger Q factors predicted in Ref. [16] and by our own modelling.

The structure is a self-standing 270 nm thick membrane of SiN_x , patterned with a hexagonal lattice (period $a = 300$ nm) of holes with radius $r = 83$ nm. A *line defect* of missing holes is created to induce a waveguide. Further modifications of the lattice are made to tailor the field confinement and to ensure that the propagating mode is not leaky. Namely, a dislocation of the two half-lattices such that their relative distance is $W = 0.95\sqrt{3}a$ and inward shift of first line of holes by 39 nm (Fig.1b, inset). This optimisation is crucial in order to cope with the substantially smaller refractive index of SiN_x ($n = 1.9$) relative to semiconductors (e.g. silicon $n = 3.4$), which considerably restricts the parameter space in the design. This is a well-know issue when creating PhC optical nanostructures using low-index materials [17], [18].

The choice of this material is however motivated by its broad transparency range, extending to the visible and near UV spectral range owing to its large band gap ($> 4eV$) [19], [20] and by the fact that it can be deposited as a thin film, implying flexibility and easy integration of heterogeneous materials. It is also important to note that SiN_x is compatible with biological tissues [21].

The calculations in Fig.1a-c consider a CdSe NW (refractive index 2.85) with radius 30 nm and length $1.5 \mu m$. These values result from an optimization considering both the cavity

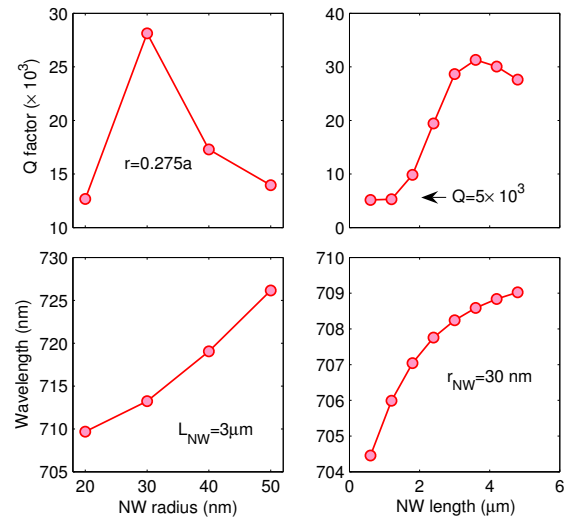


Fig. 2. Calculated dependence of the Q-factor and the resonance wavelength as a function of the geometrical parameters of the NW inserted in the PhC cavity.

Q-factor and the properties of the emitter. As apparent in Fig2, thicker NWs would induce a deeper potential well, resulting into a more abrupt confinement and, hence, a much stronger optical leakage [22], substantially decreasing the Q-factor. On the other hand, thinner and longer wires would allow better Q-factor, however the yield would decrease very fast because of the increased role of non-radiative surface recombination. Furthermore, longer NWs tend to bend during deposition and, therefore, are more difficult to process. Similar considerations are valid for NWs made of other materials, e.g. GaAs.

The calculations are made by our in-house developed 3D Finite Differences in Time Domain (FDTD) code ensuring accuracy in the calculated frequency within $\frac{\Delta f}{f} = 10^{-3}$. The resonance corresponding to a localized mode appears in the plot of the (normalized) Local Density of Optical States (LDOS), which is proportional to the spontaneous emission, calculated following Ref.[23]. We approximated the source as a dipole located at the centre of the NW and oriented along y . The Q-factor of the resonance is 5300 (i.e. linewidth = 0.13 nm), while the corresponding wavelength is 712 nm, well within the Photo Luminescence (PL) spectrum of the CdSe NWs [24]. The mode volume $V = 8.5 \times 10^{-20} m^3 = 2\left(\frac{\lambda}{n}\right)^3$ is reasonably close to the diffraction limit $\left(\frac{\lambda}{2n}\right)^3$. Hence, the overlap of the field with the NW is $\Gamma = V_{NM}V^{-1} = 0.05$, which is good, considering the small size of the emitter.

DEVICE FABRICATION

The fabrication of the structure is shown in Fig.1d-f. First, about half SiN_x layer (120 nm) is deposited on a $\langle 001 \rangle$ gallium phosphide (GaP) substrate [25], by high temperature ($360^\circ C$) and low mechanical stress Plasma Enhanced Chemical Vapor Deposition (PECVD). High quality single phase wurtzite CdSe nanowire are grown using a CVD process described in Ref.[26] with Van der Waals epitaxy on muscovite mica substrate [27]. They are then removed from their growth

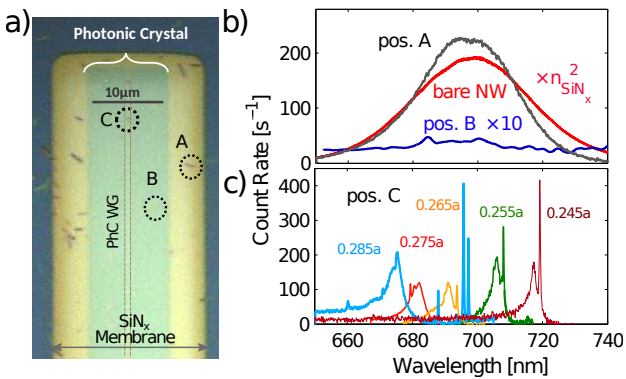


Fig. 3. Photoluminescence of randomly distributed NWs. a) optical image of the sample, circles point to the NWs whose PL is shown in panels b and c; b) NW in homogeneous SiN_x (gray, position A) and patterned SiN_x (blue, position B, multiplied by 10) and reference NW on a Quartz substrate (red); c) PL when NW crosses the PhC waveguide (position C), colour codes relate to the reduced PhC hole radius, the width of the twin narrow peaks (cyan line) is about 300 pm. The vertical axis in panels b and c can be compared quantitatively.

substrate by placing them in an ethanol solution and then in an ultrasonic bath for a few seconds [28]. The solution is then dropped on the SiN_x layer and the solvent is removed by heating at 110°C.

The NWs are further cladded by a 150 nm thick layer of SiN_x (Fig.1e), which allows to protect the NW and to symmetrize the structure. At this stage, we have not taken any specific measure to control the position of the NWs, although we point out that several techniques have been proposed[29] for the transfer and the deterministic placement of NWs on a planar substrate, for instance using nano combing [30], the Langmuir-Blodgett technique, Optical Trapping, Contact Printing, and others. Thus, the buried NWs are spatially mapped by detecting the induced relief at the surface using AFM (scanning rate 0.1 Hz, in-plane resolution 22 nm/pixel) on an area encompassing alignment marks and several NWs. The position and the angle of each NW are retrieved relative to the alignment marks (Fig.1f). Only a subset of the detected NW is retained for the fabrication of the device, according to their diameter, $50nm \pm 15nm$ (out of a broader distribution: 35 to 130 nm) and their length, chosen to be close to $1.5 \mu m$, since longer wires tend to bend during evaporation.

Then, PhC are fabricated following a fairly standard sequence of positive resist (PMMA-A4, thickness 200 nm) exposure by electron beam lithography (NANOBEAM NB4), and reactive ion etching of the SiN_x layer (Fig.1g) using a CHF_3/O_2 mixture [31]. The last step is the wet chemical etching of the GaP substrate [32] under the SiN_x Photonic Crystal in order to obtain a self-standing membrane, providing the required refractive index contrast below the structure.

The finalized device is shown in Fig.1e. As apparent in the inset, the alignment of the NW with the PhC is very good. About one hundred of these have been fabricated in a single run. On average over the investigated devices, the positioning and angular errors are 53 nm and 0.1° respectively.

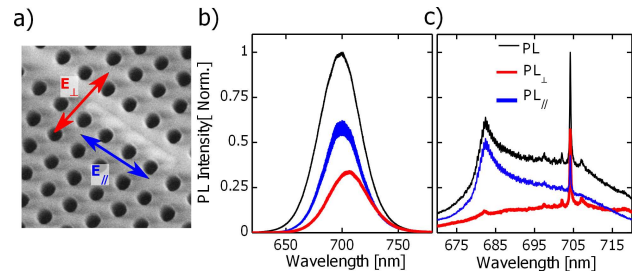


Fig. 4. Identification of the cavity mode. a) SEM image of the PhC cavity (radius $0.285a$) aligned to a NW (sample 5). The parallel ($//$) or perpendicular (\perp) alignment of the analyser is referred to the waveguide axis; b) PL of reference NW on the Quartz substrate; c) PL of the NW 5, colour code is the same as in b) and refers to the polarization.

LUMINESCENCE OF NANOWIRES EMBEDDED IN A PHC MEMBRANE

In order to appreciate the benefit of spatial alignment, it is worth investigating devices fabricated following the same procedure, except that the NWs are not aligned into the PhC cavity (e.g. the NW labelled as A in Fig.3a). The micro-Photo Luminescence (PL) is performed using a commercial equipment (Renishaw), under continuous wave pumping and using the 514 nm line of the Argon laser. A nearly diffraction-limited spot size is obtained using a $63\times$ and $N.A. = 0.95$ microscope objective. The pump is circularly polarized, in order to average over the absorption anisotropy of the NWs [33], [34].

First, we point out that embedding the NWs in SiN_x does not alter their emission properties substantially (besides the trivial effect on the collection efficiency). This is apparent in Fig.3b, where the PL spectra of the NWs, located outside the PhC area (labelled as A in Fig.3a) and of the reference NW lying on a Quartz substrate, are very similar: both centred at about 700 nm and about 30 nm broad. Although an accurate quantitative comparison is not easy, because the PL yield varies from NW to NW, it is apparent that the PL is strongly reduced by about 2 orders of magnitude, when the NW is located inside the PhC (position labelled as B). This is way larger than any possible fluctuation in the PL of different NWs. This result is reproduced systematically and is consistent with established literature on the inhibition of the spontaneous emission in PhC [35].

The PL spectrum is drastically different when the NW crosses the PhC waveguide (Fig.3c), revealing peaks which are correlated with the radius of the PhC holes as expected (the larger the radius, the shorter the wavelength). Importantly, the PL is comparable in intensity as in the case of NWs embedded into a homogeneous SiN_x layer.

The strong modification of the PL spectra of emitters embedded in the PhC waveguides is due to the strongly dispersive and large LDOS [36]. The narrow peaks ($\Delta\lambda \approx 300$ pm) correspond to the defect modes (lower in energy) induced by the NW in the PhC waveguide. Thus, the perturbation is enough to induce a resonant mode with spectral position mainly dictated by the PhC geometry, even if the position of the NW relative to the waveguide is not controlled.

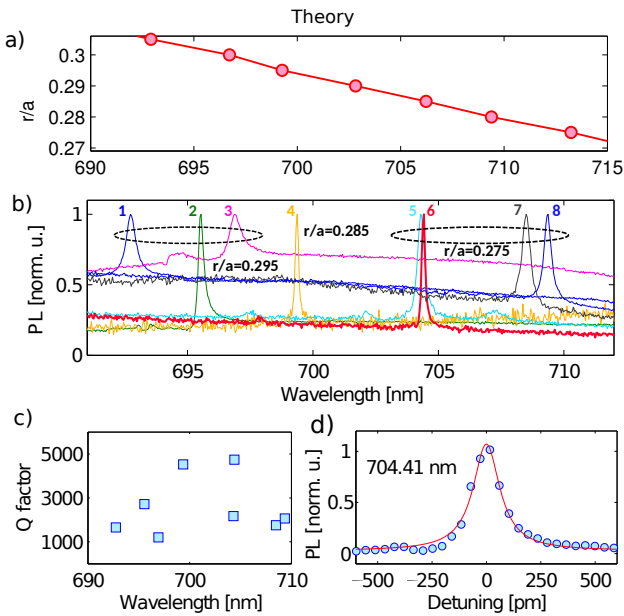


Fig. 5. a) Calculated dependence of the resonant peak as the radius of the holes in decrease. b-c) Comparison of the emission properties of sample 1 to sample 8. b) ensemble view, dashed circles denotes a common radius for the PhC holes; c) spectral width of the peak (Q factor); d) detailed lineshape and Lorentzian fit (sample 6), the resolution of the instrument is 40 pm. The PL is collected perpendicular to the NW axis.

EMISSION FROM CAVITY MODES IN ALIGNED STRUCTURES

The PL measurements on aligned NWs, are shown in Fig.4. In order to formally associate the expected resonant peak to the designed cavity mode, we also consider the polarization of the PL. While the emission of bare NWs on a Quartz substrate is moderately anisotropic (Fig.4b), with a larger parallel component [33], [34], [37], the shape of the PL emitted by our device reveals one broad and one narrow peaks. The broad peak, located at higher energies, inherits the polarization properties of the emitter, and might be related to the higher order mode of the PhC waveguide. The narrow peak is mainly perpendicularly polarized but still keeps a parallel component, as expected from the calculation of the radiated Far Field of the cavity mode, represented in Fig.1c. We point out that the relative strength of the two peaks is not entirely representative of the radiated power. In fact, PhC cavity mode radiates mainly at a grazing angle with the surface of the sample, and, therefore, only a small part of the emitted power is collected by the microscope objective. In contrast, the background PL is radiated much more isotropically, and, therefore, collected more efficiently. Note that it is possible to improve the directivity of the radiation from PhC cavities substantially (and thereby the collection nearly to 50%) by a controlled modification of the design [38], [39].

Here, one out of the eight devices selected for the systematic measurements is shown. These devices, which have been numbered from 1 to 8 according to the increasing peak wavelength, reveal the same polarization properties, as expected. We focus now on the properties of the cavity mode and therefore, we plot the perpendicular component of the spectra in Fig.5b. These 8 peaks relate to three different designs (hole sizes) of the

PhC and, indeed, they are clustered accordingly. There is an apparent dependence on the NW, depending primarily on its size (diameter between 30 and 90 nm) and secondly on the accuracy of its positioning (within 60 nm, except for sample 7). Interestingly, in sample 7 the NW is misplaced by exactly one lattice period, and still the PL yield is strong. This is not surprising given the spatial structure of the cavity mode (Fig.1c).

The measured Q-factors range from 1000 to 5000 (Fig.5c,d) and match well to a Lorentzian lineshape (Fig.5d). The highest Q factors are obtained for the NWs 4 and 6 (the thinnest NWs). It is also interesting to note that best placement (error is 25 nm) is achieved for sample 6. These results are consistent with FDTD calculations (Fig.3), predicting a monotonous decrease of the Q factor and a red shift as the radius of the NW increases from 20 nm to 50 nm. Also a positioning error larger than about 30 nm induces a decrease of the Q factor and a red shift. We note that the measured and calculated Q-factors and peak wavelengths are comparable, however, any quantitative analysis is problematic because of the fluctuations in the size of the wires, introducing too much uncertainty in the estimate of the internal absorption.

Figure 5 substantiates the main point of this letter, namely, that it is possible to generate a variety of wavelengths on the same chip by design. This is a fundamental property either for communications (wavelength domain multiplexing) or for labelling in biologic detection. An important aspect here is the possibility of accurately controlling the emission wavelength. First of all, in our experiment, the main source of fluctuation of the emitted wavelength (up to a few nm) was due to the spread of the size of the CdSe nanowires which we estimate to ± 30 nm based on Fig.3 and Fig.6. A narrower selection of nanowires would automatically result into emitted peaks gathering around the same wavelength, determined by the parameters of the PhC structure. After calibration of the fabrication process, the peak wavelength could be controlled within a fraction of nm, which should be accurate enough for applications. For even more accurate control, post-processing trimming techniques could be used [40], also including ALD [41], deposition of a thin layer of chalcogenides [42] or local temperature control [43].

DISCUSSION

The PL spectra in Fig. 6b reveals a 20% decrease of the linewidth as the fluence of the pump [44] is increased between 10^3 and 10^4 W/cm^2 . This indicates a moderate decrease of the internal absorption losses. Interestingly, the peak wavelength (Fig. 6c) also follows the usual red shift after minimum linewidth has been reached. However, the ratio between the total PL and the peak intensity is constant over more than three decades (Fig.6a), suggesting that the contribution of the stimulated emission is not strong enough to induce a detectable kink in the $P_{PL} - P_{pump}$ curve. On the other hand, no detectable sign of gain saturation has been observed.

A hint for understanding this behaviour comes from the dependence on the PL on the pump in Fig. 6a. A clearly

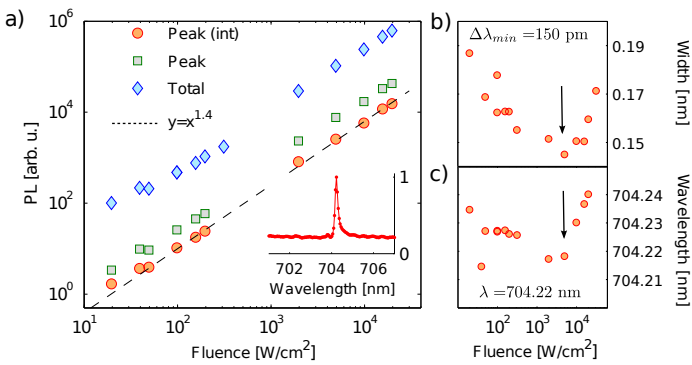


Fig. 6. PL dependence on the pump fluence, NW 6. a) total integrated PL spectra (diamonds), peak (squares) and integrated peak (circles), dotted line is the $y = x^{1.4}$ law as a guide for the eyes, spectra is in inset; b) spectral width of the peak (FWHM); c) peak spectral position and its average. PL is collected perpendicular to the NW axis.

superlinear law $PL \propto I^{1.4}$ is observed in NW 6. In another sample, we have observed a similar behavior $PL \propto I^{1.65}$ and other detailed measurement have confirmed this a general property of our NWs. This superlinear trend has been observed in narrower CdSe NWs (diameter 22 nm) under the same conditions (RT and CW pumping)[45]. The extremely detailed study carried out there points out the role of surface defects.

More precisely, fast hole trapping results into a linear dependence of the hole population on the pumping rate at intermediate pumping levels (which covers our parameter space entirely). On the other hand, the density of electrons follows the usual square root dependence on the pump. This results into a theoretical $PL \propto I^{1.5}$ dependence of the PL on the pump level, which is consistent with our findings. The main implication here is a strong quenching of the quantum yield, which we extrapolated to our case to decrease the gain by nearly an order of magnitude. According to this model, at higher pumping rate the dependence would become linear, indicating the saturation of fast traps and the increase of the quantum yield, but we have not observed any change of the slope until a maximum fluence level of 20 kW/cm^2 . Although our wires are thicker than in Ref. [45], their behaviour is strikingly similar, suggesting a more important role of surface states, possibly due to the encapsulation in an SiN matrix.

We note that lasing has been observed in recent experiments on CdSe NWs [24]. There, random lasing has been observed with a minimum threshold of about 200 kW/cm^2 . This said, the measurements have been performed in pulsed regime and with fairly thicker wires ($>100 \text{ nm}$). We also performed additional measurements on a single bare NW (on Quartz) and observed the onset of stimulated emission at a fluence of 100 kW/cm^2 .

Lasing of on fairly larger (200 to 500 nm) single CdSe NWs [46] has been observed at lower pump levels. This corroborates the hypothesis that surface recombination degrades the PL emission at Room Temperature substantially in our thin NWs (which is also apparent in the power

dependence of the PL signal). The use of core-shell structures, such as AlGaAs/GaAs [47], [48], or GaAs/GaP [49] could greatly help in achieving efficient lasing. Also, the Telecom spectral domain could be addressed by suitable choice of the III-V alloy. Interestingly, the β -factor of our device is estimated based on the mode volume to be about 0.1, using formula in Ref. [50]. This is a typical number for nanolasers. The required material gain at threshold is estimated to about 300 cm^{-1} , which is well within reach. At last, we note that in a very recent paper[51], lasing has been achieved at cryogenic temperatures in the hybrid silicon PhC structures including a fairly sophisticated NW involving several QWs. This shows that NW technology is steadily improving and would provide versatile and ultra efficient sources once combined with convenient optical cavities.

CONCLUSIONS

We have demonstrated a novel approach to the heterogeneous integration of semiconductor nanowires in a small optical cavity. The resonant optical field is self aligned around the nanowire, resulting into an efficient coupling. The key aspect of this approach is that the cavity is fabricated after the transfer of the nanowires on the substrate and, consequently, can be accurately aligned on it. This allows for the fabrication of hundreds of samples in a single processing run. Our technique could be combined with the deterministic positioning of nanowires which would address large scale fabrication. We show that the photoluminescence, hence the emission wavelength is controlled by the cavity mode, which allows for the generation of multiple wavelengths with fairly narrow peaks (150 pm) on the same optical chip. The narrow linewidth results from a cavity Q-factor as large as 5000, in spite of the limited refractive index contrast available with silicon nitride. Larger Q could be achieved if thinner and longer wires could be used. Lasing has not been achieved at the moderate pumping level used for characterization (20 kW/cm^2), but it should be within reach. Furthermore, the use of core-shell nanowire structures should allow efficient light emission, while the collection efficiency can be improved by design. For some applications, such light sources could be easily separated from their substrate and attached as wavelength-labelled markers to suitable targets.

ACKNOWLEDGMENT

Authors thank C. Couteau and C. Diederichs for valuable discussions, D. Thenot for help on the SiN depositions, S. Xavier for help on the e-beam lithography and B. Servet for helping with the PhotoLuminescence set-up. Q.X. gratefully acknowledges the financial support from Singapore National Research Foundation via NRF Investigatorship Award (NRF-NRFI2015-03), and Ministry of Education via Three Tier2 grants (MOE2011-T2-2-051, MOE2012-T2-2-086 and MOE2013-T2-1-049). C.S. acknowledges financial support of the Singapore Ministry of Education (MOE2013-T2-1-044).

REFERENCES

- [1] M. T. Hill and M. C. Gather, "Advances in small lasers," *Nature Photonics*, vol. 8, no. 12, pp. 908–918, Nov. 2014. [Online]. Available: <http://www.nature.com/doi/10.1038/nphoton.2014.239>
- [2] L. He, K. Ozdemir, J. Zhu, W. Kim, and L. Yang, "Detecting single viruses and nanoparticles using whispering gallery microlasers," *Nature Nanotechnology*, vol. 6, no. 7, pp. 428–432, Jun. 2011. [Online]. Available: <http://www.nature.com/doi/10.1038/nnano.2011.99>
- [3] J. M. Gérard, B. Sermage, B. Gayral, B. Legrand, E. Costard, and V. Thierry-Mieg, "Enhanced spontaneous emission by quantum boxes in a monolithic optical microcavity," *Phys. Rev. Lett.*, vol. 81, pp. 1110–1113, Aug 1998. [Online]. Available: <http://link.aps.org/doi/10.1103/PhysRevLett.81.1110>
- [4] M. Fujita, R. Ushigome, and T. Baba, "Continuous wave lasing in gainsp microdisk injection laser with threshold current of $40\mu\text{A}$," *Electronics Letters*, vol. 36, no. 9, p. 1, 2000.
- [5] J. B. Khurgin, "How to deal with the loss in plasmonics and metamaterials," *Nature Nanotechnology*, vol. 10, no. 1, pp. 2–6, Jan. 2015. [Online]. Available: <http://www.nature.com/doi/10.1038/nnano.2014.310>
- [6] B. Ji, E. Giovanelli, B. Habert, P. Spinicelli, M. Nasilowski, X. Xu, N. Lequeux, J.-P. Hugonin, F. Marquier, J.-J. Greffet, and B. Dubertret, "Non-blinking quantum dot with a plasmonic nanoshell resonator," *Nature Nanotechnology*, vol. 10, no. 2, pp. 170–175, Jan. 2015. [Online]. Available: <http://www.nature.com/doi/10.1038/nnano.2014.298>
- [7] Z. Zhang and M. Qiu, "Small-volume waveguide-section high Q microcavities in 2d photonic crystal slabs," *Optics Express*, vol. 12, no. 17, p. 3988, 2004. [Online]. Available: <https://www.osapublishing.org/oe/abstract.cfm?uri=oe-12-17-3988>
- [8] K. Nozaki, S. Kita, and T. Baba, "Room temperature continuous wave operation and controlled spontaneous emission in ultrasmall photonic crystal nanolaser," *Optics Express*, vol. 15, no. 12, pp. 7506–7514, 2007.
- [9] K. Takeda, T. Sato, T. Fujii, E. Kuramochi, M. Notomi, K. Hasebe, T. Kakitsuka, and S. Matsuo, "Heterogeneously integrated photonic-crystal lasers on silicon for on/off chip optical interconnects," *Optics Express*, vol. 23, no. 2, pp. 702–708, 2015. [Online]. Available: <http://www.osapublishing.org/abstract.cfm?uri=oe-23-2-702>
- [10] Y. Halioua, A. Bazin, P. Monnier, T. J. Karle, G. Roelkens, I. Sagnes, R. Raj, and F. Raineri, "Hybrid iii-v semiconductor/silicon nanolaser," *Opt. Express*, vol. 19, no. 10, pp. 9221–9231, May 2011. [Online]. Available: <http://www.opticsexpress.org/abstract.cfm?URI=oe-19-10-9221>
- [11] J. Heo, W. Guo, and P. Bhattacharya, "Monolithic single gan nanowire laser with photonic crystal microcavity on silicon," *Applied Physics Letters*, vol. 98, no. 2, p. 021110, 2011.
- [12] I. Fushman, D. Englund, and J. Vučković, "Coupling of pbs quantum dots to photonic crystal cavities at room temperature," *Applied Physics Letters*, vol. 87, no. 24, p. 241102, 2005.
- [13] M. D. Birowosuto, A. Yokoo, G. Zhang, K. Tateno, E. Kuramochi, H. Taniyama, M. Takiguchi, and M. Notomi, "Movable high-Q nanoresonators realized by semiconductor nanowires on a Si photonic crystal platform," *Nature Materials*, vol. 13, no. 3, pp. 279–285, Feb. 2014. [Online]. Available: <http://www.nature.com/doi/10.1038/nmat3873>
- [14] A. Badolato, K. Hennessy, M. Atatüre, J. Dreiser, E. Hu, P. M. Petroff, and A. Imamoglu, "Deterministic coupling of single quantum dots to single nanocavity modes," *Science*, vol. 308, no. 5725, pp. 1158–1161, 2005.
- [15] S. Strauf and F. Jahnke, "Single quantum dot nanolaser," *Laser & Photonics Reviews*, vol. 5, no. 5, pp. 607–633, 2011.
- [16] S. Sergent, M. Takiguchi, H. Taniyama, A. Shinya, E. Kuramochi, and M. Notomi, "Design of nanowire-induced nanocavities in grooved 1d and 2d sin photonic crystals for the ultra-violet and visible ranges," *Optics Express*, vol. 24, no. 23, pp. 26 792–26 808, 2016.
- [17] M. Barth, J. Kouba, J. Stingl, B. Lochel, and O. Benson, "Modification of visible spontaneous emission with silicon nitride photonic crystal nanocavities," *Optics Express*, vol. 15, no. 25, pp. 17 231–17 240, 2007. [Online]. Available: <http://www.osapublishing.org/oe/fulltext.cfm?uri=oe-15-25-17231id=148387>
- [18] I. Bayn and J. Salzman, "Ultra high-Q photonic crystal nanocavity design: The effect of a low- slab material," *Optics Express*, vol. 16, no. 7, p. 4972, Mar. 2008. [Online]. Available: <https://www.osapublishing.org/oe/abstract.cfm?uri=oe-16-7-4972>
- [19] J. Milek and M. Neuberger, *Handbook of Electronic Materials*, 1971.
- [20] A. R. Zanatta and I. B. Gallo, "The thermo optic coefficient of amorphous sin films in the near-infrared and visible regions and its experimental determination," *Applied Physics Express*, vol. 6, no. 4, 2013.
- [21] H. Gao, R. Luginbuhl, and H. Sigrist, "Bioengineering of silicon nitride," *Sensors and Actuators B: Chemical*, vol. 38, no. 1-3, pp. 38–41, Jan. 1997. [Online]. Available: <http://linkinghub.elsevier.com/retrieve/pii/S0925400596021259>
- [22] Y. Akahane, T. Asano, B.-S. Song, and S. Noda, "High-Q photonic nanocavity in a two-dimensional photonic crystal," *Nature*, vol. 425, no. 6961, pp. 944–947, Oct. 2003. [Online]. Available: <http://www.nature.com/doi/10.1038/nature02063>
- [23] Y. Xu, J. S. Vučković, R. K. Lee, O. J. Painter, A. Scherer, and A. Yariv, "Finite-difference time-domain calculation of spontaneous emission lifetime in a microcavity," *J. Opt. Soc. Am. B*, vol. 16, no. 3, pp. 465–474, Mar 1999.
- [24] R. Chen, M. I. Bakti Utama, Z. Peng, B. Peng, Q. Xiong, and H. Sun, "Excitonic Properties and Near-Infrared Coherent Random Lasing in Vertically Aligned CdSe Nanowires," *Advanced Materials*, vol. 23, no. 11, pp. 1404–1408, Mar. 2011. [Online]. Available: <http://doi.wiley.com/10.1002/adma.201003820>
- [25] "This avoids background luminescence in the spectral range of interest."
- [26] M. I. B. Utama, Z. Peng, R. Chen, B. Peng, X. Xu, Y. Dong, L. M. Wong, S. Wang, H. Sun, and Q. Xiong, "Vertically Aligned Cadmium Chalcogenide Nanowire Arrays on Muscovite Mica: A Demonstration of Epitaxial Growth Strategy," *Nano Letters*, vol. 11, no. 8, pp. 3051–3057, Aug. 2011. [Online]. Available: <http://pubs.acs.org/doi/abs/10.1021/nl1034495>
- [27] M. I. Bakti Utama, Q. Zhang, J. Zhang, Y. Yuan, F. J. Belarre, J. Arbiol, and Q. Xiong, "Recent developments and future directions in the growth of nanostructures by van der waals epitaxy," *Nanoscale*, vol. 5, pp. 3570–3588, 2013. [Online]. Available: <http://dx.doi.org/10.1039/C3NR34011B>
- [28] F. Patolsky, G. Zheng, and C. M. Lieber, "Fabrication of silicon nanowire devices for ultrasensitive, label-free, real-time detection of biological and chemical species," *Nature Protocols*, vol. 1, no. 4, pp. 1711–1724, Nov. 2006. [Online]. Available: <http://www.nature.com/doi/10.1038/nprot.2006.227>
- [29] Y. S. Lele Peng and G. Yu, "Self-assembly and organization of nanowires," *Semiconductor Nanowires: Materials, Synthesis, Characterization and Applications*, p. 149, 2015.
- [30] J. Yao, H. Yan, and C. M. Lieber, "A nanoscale combing technique for the large-scale assembly of highly aligned nanowires," *Nature nanotechnology*, vol. 8, no. 5, pp. 329–335, 2013.
- [31] C. Gatzert, A. W. Blakers, P. N. K. Deenapanray, D. Macdonald, and F. D. Auret, "Investigation of reactive ion etching of dielectrics and Si in CHF₃O₂ or CHF₃Ar for photovoltaic applications," *Journal of Vacuum Science & Technology A: Vacuum, Surfaces, and Films*, vol. 24, no. 5, p. 1857, 2006. [Online]. Available: <http://scitation.aip.org/content/avs/journal/jvsta/24/5/10.1116/1.2333571>
- [32] L. R. Plauger, "Controlled Chemical Etching of GaP," *Journal of The Electrochemical Society*, vol. 121, no. 3, p. 455, 1974. [Online]. Available: <http://jes.ecsdl.org/cgi/doi/10.1149/1.12401837>
- [33] C. Wilhelm, A. Larrue, X. Dai, D. D. Migas, and C. Soci, "Anisotropic Photonic Properties of III-V Nanowires in the Zinc-Blende and Wurtzite Phase," *Nanoscale*, vol. 4, no. 5, pp. 1446–54, Mar. 2012. [Online]. Available: <http://www.ncbi.nlm.nih.gov/pubmed/22327202>
- [34] H. Ruda and a. Shik, "Polarization-sensitive optical phenomena in semiconducting and metallic nanowires," *Physical Review B*, vol. 72, no. 11, p. 115308, Sep. 2005. [Online]. Available: <http://link.aps.org/doi/10.1103/PhysRevB.72.115308>
- [35] M. Fujita, "Simultaneous Inhibition and Redistribution of Spontaneous Light Emission in Photonic Crystals," *Science*, vol. 308, no. 5726, pp. 1296–1298, May 2005. [Online]. Available: <http://www.sciencemag.org/cgi/doi/10.1126/science.1110417>
- [36] G. Lecamp, P. Lalanne, and J. P. Hugonin, "Very large spontaneous-emission β factors in photonic-crystal waveguides," *Phys. Rev. Lett.*, vol. 99, p. 023902, Jul 2007. [Online]. Available: <http://link.aps.org/doi/10.1103/PhysRevLett.99.023902>
- [37] A. Mishra, L. V. Titova, T. B. Hoang, H. E. Jackson, L. M. Smith, J. M. Yarrison-Rice, Y. Kim, H. J. Joyce, Q. Gao, H. H. Tan, and C. Jagadish, "Polarization and temperature dependence of photoluminescence from zincblende and wurtzite InP nanowires," *Applied Physics Letters*, vol. 91, no. 26, p. 263104, 2007. [Online]. Available: <http://scitation.aip.org/content/aip/journal/apl/91/26/10.1063/1.2828034>
- [38] N.-V.-Q. Tran, S. Combré, and A. De Rossi, "Directive emission from high-Q photonic crystal cavities through band folding," *Phys.*

- Rev. B*, vol. 79, no. 4, p. 41101, 2009. [Online]. Available: <http://link.aps.org/doi/10.1103/PhysRevB.79.041101>
- [39] N.-V.-Q. Tran, S. Combr e, P. Colman, A. De Rossi, and T. Mei, "Vertical high emission in photonic crystal nanocavities by band-folding design," *Physical Review B*, vol. 82, no. 7, p. 075120, Aug. 2010. [Online]. Available: <http://link.aps.org/doi/10.1103/PhysRevB.82.075120>
- [40] J. Schrauwen, D. Van Thourhout, and R. Baets, "Trimming of silicon ring resonator by electron beam induced compaction and strain," *Optics Express*, vol. 16, no. 6, p. 3738, Mar. 2008. [Online]. Available: <https://www.osapublishing.org/oe/abstract.cfm?uri=oe-16-6-3738>
- [41] C. J. Chen, C. A. Husko, I. Meric, K. L. Shepard, C. W. Wong, W. M. J. Green, Y. A. Vlasov, and S. Assefa, "Deterministic tuning of slow-light in photonic-crystal waveguides through the C and L bands by atomic layer deposition," *Applied Physics Letters*, vol. 96, no. 8, p. 081107, 2010. [Online]. Available: <http://scitation.aip.org/content/aip/journal/apl/96/8/10.1063/1.3308492>
- [42] A. Canciamilla, S. Grillanda, F. Morichetti, C. Ferrari, J. Hu, J. D. Musgraves, K. Richardson, A. Agarwal, L. C. Kimerling, and A. Melloni, "Photo-induced trimming of coupled ring-resonator filters and delay lines in As₂S₃ chalcogenide glass," *Optics Letters*, vol. 36, no. 20, p. 4002, Oct. 2011. [Online]. Available: <https://www.osapublishing.org/ol/abstract.cfm?uri=ol-36-20-4002>
- [43] M. J. Strain, C. Lacava, L. Meriggi, I. Cristiani, and M. Sorel, "Tunable Q-factor silicon microring resonators for ultra-low power parametric processes," *Optics Letters*, vol. 40, no. 7, p. 1274, Apr. 2015. [Online]. Available: <http://www.opticsinfobase.org/abstract.cfm?URI=ol-40-7-1274>
- [44] "the estimated area for the focusing spot is 1.5 μm^2 ."
- [45] F. Vietmeyer, P. a. Frantsuzov, B. Janko, and M. Kuno, "Carrier recombination dynamics in individual CdSe nanowires," *Physical Review B - Condensed Matter and Materials Physics*, vol. 83, no. 11, pp. 1–10, 2011.
- [46] Y. Xiao, C. Meng, P. Wang, Y. Ye, H. Yu, S. Wang, F. Gu, L. Dai, and L. Tong, "Single-Nanowire Single-Mode Laser," *Nano Letters*, vol. 11, no. 3, pp. 1122–1126, Mar. 2011. [Online]. Available: <http://pubs.acs.org/doi/abs/10.1021/nl1040308>
- [47] B. Mayer, D. Rudolph, J. Schnell, S. Morktter, J. Winnerl, J. Treu, K. Miller, G. Bracher, G. Abstreiter, G. Koblmmler, and J. J. Finley, "Lasing from individual GaAs-AlGaAs core-shell nanowires up to room temperature," *Nature Communications*, vol. 4, Dec. 2013. [Online]. Available: <http://www.nature.com/doi/abs/10.1038/ncomms3931>
- [48] D. Saxena, S. Mokkapatil, P. Parkinson, N. Jiang, Q. Gao, H. H. Tan, and C. Jagadish, "Optically pumped room-temperature GaAs nanowire lasers," *Nature Photonics*, vol. 7, no. 12, pp. 963–968, Nov. 2013. [Online]. Available: <http://www.nature.com/doi/abs/10.1038/nphoton.2013.303>
- [49] G. Priante, G. Patriarche, F. Oehler, F. Glas, and J.-C. Harmand, "Abrupt GaP/GaAs Interfaces in Self-Catalyzed Nanowires," *Nano Letters*, p. 150805132220009, Aug. 2015. [Online]. Available: <http://pubs.acs.org/doi/abs/10.1021/acs.nanolett.5b02224>
- [50] A. Larrue, C. Wilhelm, G. Vest, S. Combr e, A. De Rossi, and C. Soci, "Monolithic integration of III-V nanowire with photonic crystal microcavity for vertical light emission," *Optics express*, vol. 20, no. 7, pp. 7758–7770, 2012. [Online]. Available: <http://www.osapublishing.org/aop/fulltext.cfm?uri=oe-20-7-7758>
- [51] A. Yokoo, M. Takiguchi, M. D. Birowosuto, K. Tateno, G. Zhang, E. Kuramochi, A. Shinya, H. Taniyama, and M. Notomi, "Subwavelength nanowire lasers on a silicon photonic crystal operating at telecom wavelengths," *ACS Photonics*, vol. 4, no. 2, pp. 355–362, 2017.

BIOGRAPHIES



Christophe E. Wilhelm MS in electrical engineering at the Institut d'Optique and Ecole Sup rieure de Physique et de Chimie Industrielles, in France. PhD in 2015 from Nanyang Technological University (NTU) in Singapore and from Ecole Polytechnique in France. The focus of his doctoral research was the development of novel nanoscale optical sources.



M. Iqbal Bakti Utama received a bachelor degree in physics from Nanyang Technological University (NTU), Singapore in 2012. His thesis dealt with the development of epitaxial synthesis strategy for semiconductor nanowires and other non-planar nanostructures. He then conducted research as a Project Officer in the laboratory of Prof. Qihua Xiong at NTU between 2012–2015. Presently, he is pursuing a Ph.D. degree at the University of California, Berkeley, United States. His current research focuses on observing and controlling emerging phenomena

in 2D layered materials by combining experimental toolbox from laser spectroscopy and device characterizations.



Ga lle Lehoucq Graduated at Ecole Centrale de Lille in electrical engineering in 2006, she joined the LPICM (Laboratoire de Physique des Interfaces et des Couches Minces, Ecole Polytechnique, Palaiseau) and obtained in 2010 her Ph.D. degree in physics and material science. Since 2010, she is a research scientist in Thales Research and Technology, Palaiseau, France. Her work is focused on thin-films patterning, from the micro to the nanoscale. She is currently working on the fabrication of nanostructured optical devices, including sub-wavelength

optics and photonic crystals.



Qihua Xiong received in 2006 his Ph.D. degree in Materials Science from the Pennsylvania State University under the supervision of Professor Peter C. Eklund. From 2006 to 2009, he was a postdoctoral researcher at Harvard University. In 2009 he joined the Nanyang Technological University in Singapore, holding a joint appointment between the School of Physical and Mathematical Sciences and School of Electrical and Electronic Engineering. He is now Professor of Physics and Electrical Engineering, in the School of Physical and Mathematical Sciences

and School of Electrical and Electronic Engineering, at Nanyang Technological University, Singapore.



Cesare Soci received Laurea and Ph.D. degrees in Physics from the University of Pavia, in 2000 and 2005. He was a postdoctoral researcher from 2005 to 2006 at the Center for Polymers and Organic Solids of the University of California, Santa Barbara, and from 2006 to 2009 at the Electrical and Computer Engineering Department of the University of California, San Diego. In 2009 he joined the Nanyang Technological University in Singapore, where he currently holds a joint appointment between the Schools of Physical and Mathematical

Sciences (SPMS) and Electrical and Electronic Engineering (EEE), and he is the deputy director of the Centre for Disruptive Photonic Technologies. His research embraces several areas of nanoelectronics and nanophotonics, including organic semiconductors, nanowires and plasmonic materials.



Daniel Dolfi Graduated from the Ecole Supérieure d'Optique, Orsay, (1986), received the PhD degree from University Paris XI Orsay (1993) and the Habilitation à Diriger des Recherches in 2008. He joined Thomson-CSF Corporate Research Laboratory (now TRT-France), in 1986 where he is currently Director of the Physics Dept. of TRT. His main research interests include optoelectronic generation and processing of microwave and THz signals, non-linear optics in fibers, opto-electronic devices (down to nano-scale) and sub-systems (e.g. sensors),

active optronic systems (lidars and imaging systems), superconductor based microwave devices and graphene based optoelectronics. Dr Dolfi has about 80 publications in refereed journals, about 130 communications in international conferences and about 70 registered patents. He is EOS Fellow and OSA Fellow and IEEE member.



Alfredo De Rossi PhD 2002 Universit Roma Tre, MS, 1997 in electrical engineering Università La Sapienza, A. De Rossi is with TRT (THALES Research Center in Palaiseau) since 2000. His expertise is in nonlinear and integrated optics, with particular emphasis on photonic crystals and other sub-wavelength photonic structures. His current focus is in the ultrafast nonlinear processes at chip scale, such as all-optical switching, bistability, parametric generation and conversion. He is author of about 100 journal articles and holds more than 10 patents.



Sylvain Combrié MS from Ecole Nationale Supérieure des Télécommunications (ENST) and Paris VI university in 2002. He received his PhD in 2006 from Paris XI University on the design and fabrication of Photonic Crystal (PhC) structures for optical signal processing. The highlight of his PhD work was the achievement of the highest Q-factors for PhC cavities on III-V semiconductors, the crucial milestone for the development of advanced photonic III-V nanostructures. He is the author of 7 patents and more than 65 publications.